

of stable polymers.⁹ This indicates that the peaks in the spectra (Figure 1) are a fair representation of the distribution of masses of the degradation products II.

We propose that the ions observed in the FD mass spectra correspond to the ionized products of the first step in the reported two-stage degradation of poly(1-butene sulfone) and poly(propene sulfone).⁴ β -Hydrogen shifts^{2,3} to sulfone groups would produce products with the required formula (shown in II). β -Hydrogen shifts have also been suggested to occur in poly(olefin sulfones) by Wellisch et al.¹⁹ If β -hydrogen shifts occurred at the temperatures in question in the regular poly(olefin sulfone) structure as depicted in I, it is difficult to explain why further degradation is not induced on raising the heating current from 19 to 25 mA. We conclude that the degradation products II observed in our experiments are the result of the rupture of weak links in the polymer chain.

Acknowledgment. We thank the Australian Research Grants Scheme for supporting this work.

Registry No. Poly(1-butene sulfone) (SRU), 77464-94-9; (1-butene)-(sulfur dioxide) (copolymer), 25104-10-3; poly(propene sulfone) (SRU), 77450-82-9; (propene)-(sulfur dioxide) (copolymer), 30475-44-6.

References and Notes

- (1) Dainton, F. S.; Ivin, K. J. *Proc. R. Soc. London, Ser. A* **1952**, A212, 207.
- (2) Naylor, M. A.; Anderson, A. W. *J. Am. Chem. Soc.* **1954**, 76, 3962.
- (3) Bowmer, T. N.; O'Donnell, J. H. *Polym. Degrad. Stab.* **1981**, 3, 87.
- (4) Bowden, M. J.; Thompson, L. F.; Robinson, W.; Biolsi, M. *Macromolecules* **1982**, 15, 1417.
- (5) Beckey, H. D. *Principles of Field Ionization and Field Desorption Mass Spectrometry*; Pergman: Oxford, 1977.
- (6) Neumann, G. M.; Rogers, D. E.; Derrick, P. J.; Paterson, P. J. *K. J. Phys. D: Appl. Phys.* **1980**, 13, 455.
- (7) Darcy, M. G.; Rogers, D. E.; Derrick, P. J. *Int. J. Mass. Spectrom. Ion Phys.* **1978**, 27, 335.
- (8) Cullis, P. G.; Neumann, G. M.; Rogers, D. E.; Derrick, P. J. *Adv. Mass Spectrom.* **1980**, 8, 1729.
- (9) Neumann, G. M.; Cullis, P. G.; Derrick, P. J. *Z. Naturforsch., A* **1980**, 35a, 1090.
- (10) Beckey, H. D.; Schulten, H.-R. In *Mass Spectrometry, Part A, Practical Spectroscopy Series*; McEwen, C. N., Merritt, C., Eds.; Marcel Dekker: New York, 1979; Vol. 3, pp 145-264.
- (11) Schulten, H.-R.; Dussell, H. J. *J. Anal. Appl. Pyrol.* **1980/1981**, 2, 293.
- (12) Bahr, U.; Lüderwald, I.; Müller, R.; Schulten, H.-R. *Angew. Makromol. Chem.* **1984**, 120, 163.
- (13) Winkler, H. U.; Linden, B. *Org. Mass Spectrom.* **1976**, 11, 327.
- (14) Fraley, D. F.; Pedersen, L. G.; Bursey, M. M. *Int. J. Mass Spectrom. Ion Phys.* **1982**, 43, 99.
- (15) Ivin, K. J.; Rose, J. B. *Adv. Macromol. Chem.* **1968**, 1, 335.
- (16) Bowmer, T. N.; O'Donnell, J. W. *Polym. Bull. (Berlin)* **1980**, 2, 103.
- (17) Craig, A. G.; Derrick, P. J. *J. Chem. Soc., Chem. Commun.* **1985**, 891.
- (18) Derrick, P. J. In *Mass Spectrometry*; Johnstone, R. A. W., Ed.; The Royal Society of Chemistry: London, 1977; Specialist Periodical Reports Vol. 4, p 132.
- (19) Wellisch, E.; Gipstein, E.; Sweeting, O. J. *J. Appl. Polym. Sci.* **1964**, 8, 1623.

X-ray Study on Lattice Thermal Expansion of Fully Extended Aromatic Polyamide Fibers

TADAOKI II, KOHJI TASHIRO,
MASAMICHI KOBAYASHI,* and
HIROYUKI TADOKORO

Department of Macromolecular Science, Faculty of Science,
Osaka University, Toyonaka, Osaka 560, Japan.

Received January 30, 1985;

Revised Manuscript Received February 14, 1986

As is well-known, highly oriented poly(*p*-benzamide) (PBA) and poly(*p*-phenyleneterephthalamide) (PPTA)

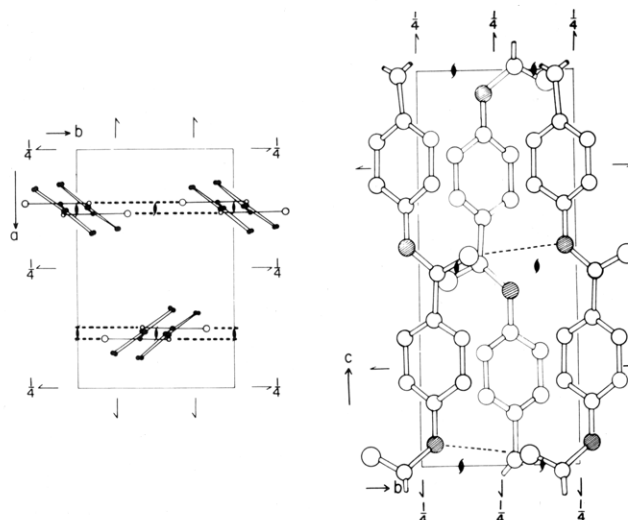


Figure 1. Crystal structure of PBA.¹²

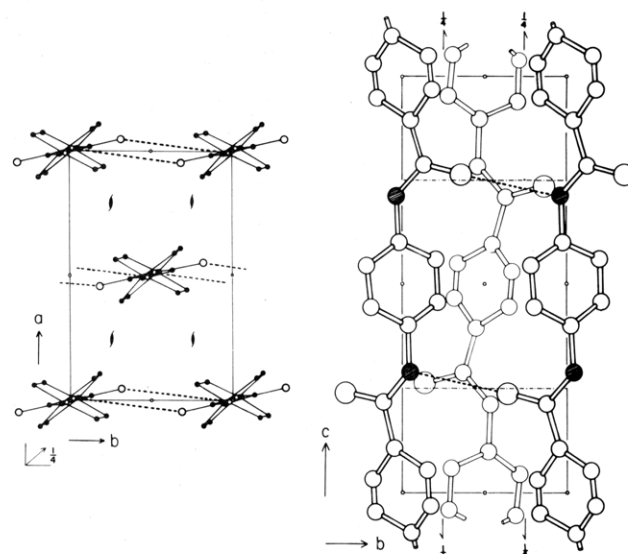


Figure 2. Crystal structure of PPTA.^{12,13}

fibers are composed of so-called fully extended rigid-rod chains.^{1,2} For these fibers macroscopic properties such as elastic modulus and thermal expansibility are expected to reflect directly the behavior of the extended chain,³⁻⁵ whereas for usual crystalline polymers consisting of flexible chains, the inherent contribution of the extended chain in the crystalline region is obscured in such macroscopic properties by the presence of more deformable noncrystalline parts, including bent or folded molecular conformations.^{6,7} Therefore, these rigid-rod polymers are suitable materials for understanding the characteristic role of the extended-chain structure in macroscopic properties.

Here we focus our attention on the problem of thermal expansion. For many crystalline polymers, including polyethylene, negative thermal expansion (thermal contraction) of the fiber period has been observed by means of X-ray diffraction and ascribed to thermal fluctuation of the molecular chain moving perpendicular to the chain axis.⁸⁻¹⁰ On the other hand, the thermal expansion behavior in the macroscopic dimension is rather complex, and its coefficient varies from positive to negative according to the sample preparation conditions and the measuring temperature.⁷ In a previous paper,¹¹ we reported thermomechanical properties of PBA and PPTA fibers and showed that these fibers exhibit a macroscopic thermal contraction of the order of 10^{-5} K^{-1} along the fiber direction. Taking into account the fully extended molecular

Table I
Crystallographic Data of Two Aromatic Polyamides^{12,13}

	PBA	PPTA
crystal system	orthorhombic	monoclinic
lattice constants	$a = 0.771$ nm $b = 0.514$ nm $c = 1.28$ nm	$a = 0.780$ nm $b = 0.519$ nm $c = 1.29$ nm $\gamma = 90^\circ$
crystal density	1.54 g/cm ³	1.50 g/cm ³

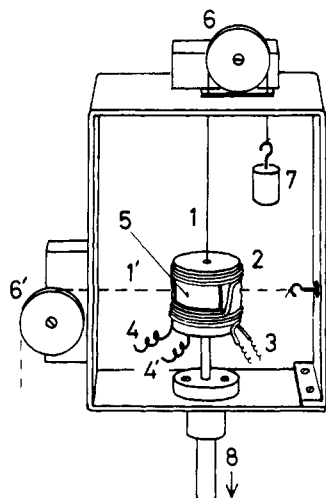


Figure 3. Sample loading system with a thermocontrolled cell: (1) sample fiber; (2) cell; (3) heater; (4, 4') thermocouple; (5) Al foil window; (6, 6') pulley; (7) weight; (8) brass rod for setting to the turning table of the X-ray diffraction system.

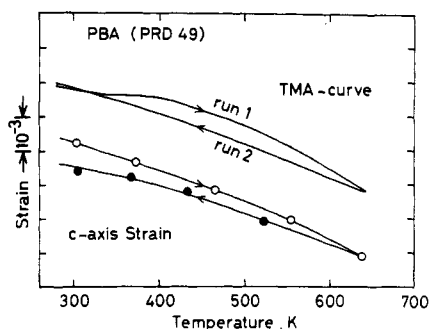


Figure 4. Temperature dependence of the c -axis strain (○ and ●) in comparison with that of bulk strain (TMA curves¹¹) for PBA.

chain structure of these fibers, we have assumed that this macroscopic thermal contraction may reflect directly the thermal fluctuation of the crystal lattice. However, as far as we know, there has been no report that deals with such a negative thermal expansion along the fiber axis for these rigid-rod polymers.

In the present paper we report experimental results on the negative thermal expansion of the c axis for PBA and PPTA along with the thermal expansion of the a and b axes measured by the X-ray diffraction method. On the basis of these experimental results, we clarify the intimate relationship between macroscopic and microscopic thermal expansion.

Experimental Section

Materials. Two sorts of ultrahigh-modulus aramide fibers produced by Du Pont have been examined, namely PRD 49 (Type I) for PBA and Kevlar 49 for PPTA. Their crystal structures^{12,13} are reproduced in Figures 1 and 2, respectively, and their crystallographic parameters are given in Table I.

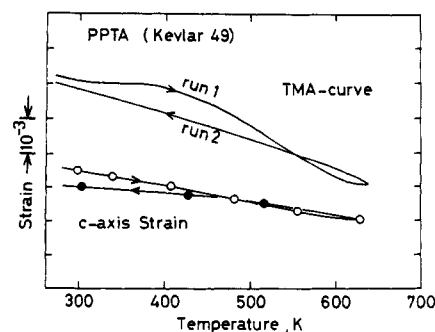


Figure 5. Temperature dependence of the c -axis strain (○ and ●) in comparison with that of bulk strain (TMA curves¹¹) for PPTA.

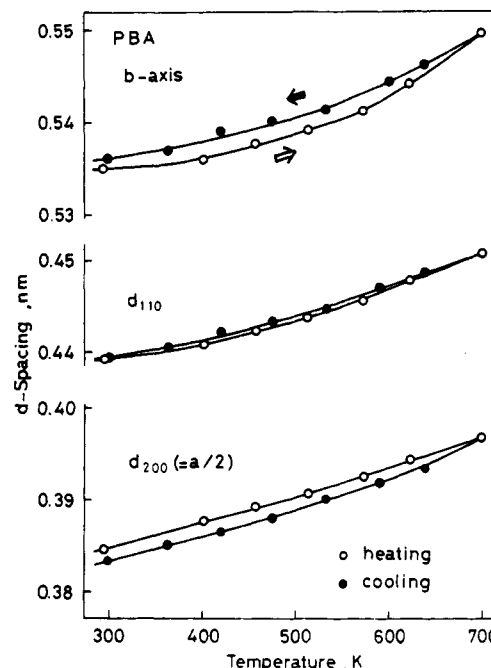


Figure 6. Temperature dependence of d spacings in the lateral direction for PBA.

X-ray Diffraction Measurement. Ni-filtered Cu $K\alpha$ radiation ($\lambda = 0.1542$ nm) through a pinhole collimator was used as an X-ray source. The diffracted beams were detected by a position-sensitive proportional counter (PSPC), which was set 30 cm from the sample position. Figure 3 illustrates the sample mounting frame with a thermocontrolled cell. The sample was tensioned slightly by a small weight. The temperature of the sample was detected by a CA thermocouple located near the center of the sample in the cell. The (004) reflection was measured with the fiber set horizontally to obtain the c -axis strain. The (110) and (200) reflections were measured in the geometry of the vertical setting of the fiber. The dimension of the b axis was estimated as $b = [d_{110}^{-2} - (2d_{200})^{-2}]^{-1/2}$. In this calculation, pseudoorthorhombic symmetry ($\gamma = 90^\circ$) is assumed for PPTA in the high-temperature condition as well as in the room-temperature condition.

Results and Discussion

Temperature Dependence of the c -Axis Dimension. Figures 4 and 5 show the temperature dependence of the c -axis strain (open and filled circles) in comparison with that of bulk strain (runs 1 and 2 of the TMA curves¹¹) for PBA and PPTA, respectively.

The open circles and run 1 are the results for the as-received samples. The filled circles and run 2 show the

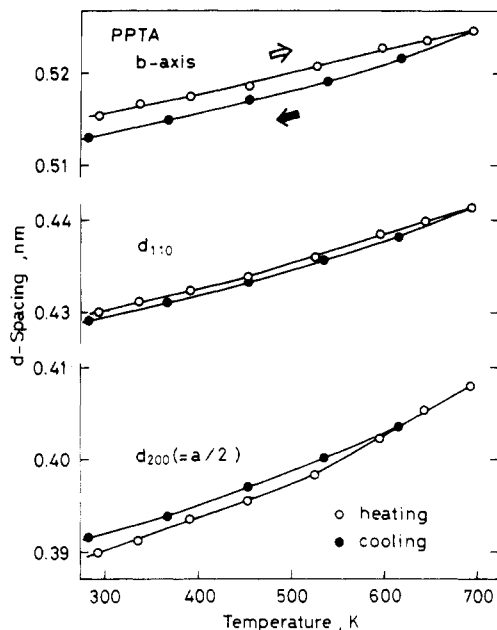


Figure 7. Temperature dependence of d spacings in the lateral direction for PPTA.

behavior of the annealed samples resulting from the heat treatment during the first heating process.

As shown in these figures, the c axis contracts with a rise of temperature for both the as-received and annealed states of PBA and PPTA. Some hysteresis is recognizable for the crystal c axis of both polymers, indicating that the c -axis dimension is slightly dependent on the sample preparation condition even for these fully extended polymers. For the annealed sample of PBA, the lattice contraction from 300 to 600 K is 0.23%; thus the average thermal expansion coefficient is estimated as $\alpha_c = -7.7 \times 10^{-6} \text{ K}^{-1}$. For the annealed sample of PPTA, the lattice contraction from 300 to 600 K is 0.087%; thus $\alpha_c = -2.9 \times 10^{-6} \text{ K}^{-1}$. These lattice contractions can be ascribed to the above-mentioned thermal fluctuation mechanism in common with many crystalline polymers. The estimated values of α_c are appreciably smaller than that of polyethylene ($-1.1 \times 10^{-5} \text{ K}^{-1}$ between 93 and 333 K).⁹ It should be noted, however, that even for these rigid-rod polymers negative contractions along the fiber axis have been observed in the same order-of-magnitude as that of the flexible-chain polymer. The difference in the α_c between PBA and PPTA will be discussed below in relation to the thermal expansions of the lateral spacings.

Some elongation is observed for the bulk dimension in the range 300–400 K of run 1, which has been ascribed to the dehydration effect.^{11,14} But such an elongation has not been observed for the c axis of the crystal lattice, and also the thermal behavior of the lattice seems uninfluenced by the presence of adsorbed water. Except for this range, the lattice and the bulk dimensions behave in parallel fashion. The bulk expansion coefficients of the annealed samples are estimated as $\alpha = -8.5 \times 10^{-6} \text{ K}^{-1}$ for PBA and $\alpha = -7.6 \times 10^{-6} \text{ K}^{-1}$ for PPTA in the range 300–600 K. The coincidence in the order of contraction between the lattice and bulk supports the fully extended or paracrystalline structure model proposed for these fibers.^{1–5} The difference between α_c and α is only about 10% for PBA and about 60% for PPTA. Therefore, such a paracrystalline concept is more appropriate for the PBA fiber.

Temperature Dependences of the Lateral Spacings. These are shown in Figures 6 and 7. The open and filled circles represent the data obtained during the heating and cooling processes, respectively. In contrast to the case of

Table II
Thermal Expansion Coefficients in the Lateral Direction^a

expansn coeff, 10^{-5} K^{-1}	temp range, K	
	300–500	500–700
PBA		
α_a	7.0	9.8
α_{110}	5.4	7.8
α_b	4.1	8.7
PPTA		
α_a	8.3	12.0
α_{110}	5.8	8.1
α_b	4.7	6.3

^a These values have been determined for the annealed states.

the c axis, the lateral spacings a , b , and d_{110} increase with a rise of temperature, giving ordinary positive thermal expansion coefficients. The slope or the thermal expansibility increases continuously with temperature for both PBA and PPTA. Our results for PPTA in Figure 7 is roughly similar to the data of Haraguchi et al.¹⁵

Table II lists the averaged thermal expansion coefficients of the lateral spacings for the annealed state in the middle (300–500 K) and high (500–700 K) temperature ranges. For both PBA and PPTA the expansion coefficient along the a axis is somewhat smaller than that along the b axis, the latter being parallel to the direction of hydrogen bonding (see Figures 1 and 2). For the PE lattice the thermal expansion has been estimated as $\alpha_a = (1-2.5) \times 10^{-4} \text{ K}^{-1}$ and $\alpha_b = 4.5 \times 10^{-5} \text{ K}^{-1}$ between 93–333 K. Disregarding the difference in the measuring range of temperature, the thermal expansion coefficient of the a axis (the direction of the largest thermal expansion) for the PE lattice is about 1.5–3 times larger than those for the aramid fibers as listed in Table II.

The above-described thermal expansion in the lateral direction has been regarded as an index of the thermal fluctuation of the molecular chain perpendicular to the chain axis, and the thermal contraction of the c axis (fiber period) is regarded as another index of such a fluctuation. In this respect, the nonnegligible difference in the magnitude of α_c between PBA and PPTA seems to rather contradict the similarity in the lateral thermal expansion. (The cross-sectional area $a \times b$ increases by 6.0% for PBA and 6.6% for PPTA from 300 to 700 K. Judging from these values, we can say that the averaged lateral thermal expansion is almost the same for PBA and PPTA, although the anisotropy in the lateral thermal expansion is considered somewhat larger for PPTA than for PBA.)

According to our theoretical consideration based on the chain fluctuation mechanism, the strain ϵ along the chain axis is approximately given by¹⁶

$$\epsilon = \frac{\sigma}{E_0} - \frac{1}{2} \sum \frac{k_B T}{\rho v^2 + \sigma}$$

The first term represents an elongation of the chain length along the chain skeleton due to the external tensile stress σ . E_0 denotes the Young's modulus at 0 K. The second term indicates the contraction due to the thermal fluctuation of the chain. The summation runs over all the transverse modes of the molecular chain. $k_B T$ originates from the time-averaged energy of each transverse mode in the high-temperature approximation, where k_B is the Boltzmann constant and T is the absolute temperature. v is the phase velocity along the chain axis. ρ is the density of the system. In general, ρv^2 depends on the intermolecular interaction, the chain conformation, and the wavenumber of the transverse mode. Roughly speaking, ρv^2 corresponds to a shear modulus for the mode with a low wavenumber. Therefore, the difference found experi-

mentally in the thermal contraction of the *c* axis between PBA and PPTA could be attributed to the difference in ρv^2 or in the anisotropic intermolecular interaction and the chain conformation between the two crystals. The thermal expansion data presented in this paper, however, are not sufficient to estimate the magnitude of ρv^2 . On the other hand, tensile property data (i.e., curves of ϵ vs. σ measured at various temperatures) will be available for the estimation of ρv^2 , as understood from the presence of the external stress σ in the above equation. Detailed experimental results on the tensile property of these fibers will be reported later.¹⁷

Registry No. PBA (SRU), 24991-08-0; PBA (homopolymer), 25136-77-0; PPTA (SRU), 24938-64-5; PPTA (copolymer), 25035-37-4.

References and Notes

- (1) Morgan, P. W. *Macromolecules* **1977**, *10*, 1831.
- (2) Kwolek, S. L.; Morgan, P. W.; Schaefer, J. R.; Gulrich, L. W. *Macromolecules* **1977**, *10*, 1390.
- (3) Yabuki, K.; Koda, H.; Endo, S.; Kajima, I.; Yukimatsu, K.; Konomi, T. *Sen'i Gakkaishi* **1978**, *34*, T-342.
- (4) Northolt, M. G.; Van Aartsen, J. J. *J. Polym. Sci., Polym. Symp.* **1977**, No. 58, 283.
- (5) Slutsker, L. I.; Utevshii, L. E.; Chereiskii, Z. Yu.; Perepelkin, K. E. *J. Polym. Sci., Polym. Symp.* **1977**, No. 58, 339.
- (6) Takayanagi, M.; Imada, K.; Kajiyama, T. *J. Polym. Sci., Part C* **1966**, *15*, 263.
- (7) Choy, C. L.; Chen, F. C.; Young, K. J. *J. Polym. Sci., Polym. Phys. Ed.* **1981**, *19*, 335.
- (8) Wakelin, J. H.; Sutherland, A.; Beck, L. R., Jr. *J. Polym. Sci.* **1960**, *42*, 139.
- (9) Davis, G. T.; Eby, R. K.; Colson, J. P. *J. Appl. Phys.* **1970**, *37*, 4316.
- (10) Kobayashi, Y.; Keller, A. *Polymer* **1970**, *11*, 114.
- (11) Ii, T.; Tashiro, K.; Kobayashi, M.; Tadokoro, H. *Macromolecules*, in press.
- (12) Hasegawa, R. K.; Chatani, Y.; Tadokoro, H., presented at the Meeting of the Crystallographic Society of Japan, Osaka, 1973; Prepr p 21.
- (13) Northolt, M. G.; Van Aartsen, J. J. *J. Polym. Sci., Polym. Lett. Ed.* **1973**, *11*, 333.
- (14) Brown, J. R.; Ennis, B. C. *Text. Res. J.* **1977**, *47*, 62.
- (15) Haraguchi, K.; Kajiyama, T.; Takayanagi, M. *Sen'i Gakkaishi* **1977**, *33*, T-535.
- (16) Ii, T.; Tashiro, K.; Kobayashi, M.; Tadokoro, H., *Macromolecules*, to be submitted.
- (17) Ii, T.; Tashiro, K.; Kobayashi, M.; Tadokoro, H., *Macromolecules*, to be submitted.

Communications to the Editor

Sequential Silyl Aldol Condensation in Controlled Synthesis of Living Poly(vinyl alcohol) Precursors[†]

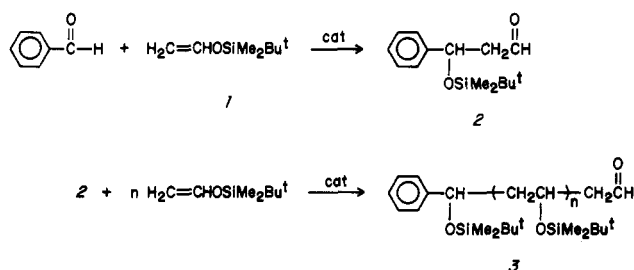
Michael addition and aldol condensation constitute an important group of organic reactions available for carbon-carbon bond formation. We recently reported application of the former to controlled synthesis of acrylic polymers.² The method, termed group-transfer polymerization (GTP), give monodisperse living³ methacrylate polymers of well-controlled molecular weight. In this communication we describe the first application of silyl aldol condensation to direct synthesis of living macromolecules whose structure and molecular weight are controlled by the initiator.

Aldehydes are known to react with silyl vinyl ethers to give silylated crossed-aldol products.⁴ Since a new aldehyde group is formed in aldol condensation of silyl vinyl ethers, continued addition of the silyl vinyl ether should give a polymer. We find that addition of a several-fold excess of silyl vinyl ether 1^{4c} to benzaldehyde as initiator gives a silylated vinyl alcohol polymer with a terminal aldehyde group (Scheme I). The molecular weight of the polymer as shown in Table I is controlled by the molar ratio of the silyl vinyl ether to the aldehyde initiator.

Unlike GTP of methyl methacrylate in which the *silyl group is transferred from the initiator to the monomer*, the polymerization of silyl vinyl ethers, hereafter referred to as *aldol-GTP*, involves a *transfer of the silyl group from monomer to initiator*. The products are stable, neutral living polymers whose hydrolytic stability depends on the bulkiness of the silyl group. In line with the well-known enhanced hydrolytic stability of *tert*-butyldimethylsilyl ethers compared to the corresponding trimethylsilyl ethers,⁵ we find that the best control of molecular weight is obtained with *tert*-butyldimethylsilyl vinyl ethers over a wide temperature range (-80 to +70 °C).⁶

A catalyst is required for the process to occur. Although

Scheme I



Lewis acids such as diisobutylaluminum chloride and titanium tetrachloride are effective (Table I, run nos. 9 and 10) as catalysts, the preferred catalysts are zinc halides (Table I, run nos. 1-7). Titanium tetrachloride gives low yields of polymer (<20%), presumably due to its depletion via exchange reactions which it is likely to undergo with silyl groups. Anionic catalysts, particularly fluoride sources such as tris(dimethylamino)sulfonium bifluoride (Table I, run no. 8), strongly coordinate not only to the incoming silyl vinyl ether but also to the backbone siloxy groups. This makes such species less efficient catalysts for the aldol-GTP than Lewis acids. Nonreactive chlorinated and nonpolar aromatic solvents are more compatible with Lewis acids than are polar solvents such as tetrahydrofuran and acetonitrile; hence, the former are preferred. In contrast to Lewis acid catalyzed GTP of methacrylates⁷ in which catalyst levels of about 10-20 mol % relative to monomer are needed for complete monomer conversion, the aldol-GTP requires much less catalyst, usually ranging from 10⁻⁴ to 10⁻² mol % relative to the silyl vinyl ether (monomer).

In general, aromatic aldehydes react more cleanly as initiators than do aliphatic aldehydes (Table I, run nos. 4, 5, and 12). Besides aldehydes, electrophiles such as benzyl halides (Table I, run no. 6) and acetals (Table I, run no. 11) can be used as initiators. Use of either 1,4-bis(bromomethyl)benzene (Scheme II) or terephthalde-

[†] Contribution No. 3852.